A comprehensive catalog of 3D parameters of front-side halo CMEs using STEREO and SOHO from 2009 to 2013

Soojeong Jang, Graduate student

Kyung Hee University, Korea

Abstract

We present a comprehensive catalog of 308 front-side halo (partial and full) CMEs from 2009 to 2013 observed by both SOHO and STEREO. This catalog includes 2D CME parameters from single spacecraft (SOHO) as well as 3D ones from multi-spacecraft. To determine the 3D CME parameters (speed, angular width, and source location), we use the STEREO CME analysis tool based on a triangulation method. In this paper, we compare between 2D and 3D CME parameters, which is the first statistical comparison between them. As a result, we find that 2D speeds tend to be about 20% underestimated when compared to 3D ones. The 3D angular width ranges from 30° to 158°, which are much smaller than the 2D angular widths with the mean value of 225°. We also find that a ratio between 3D and 2D angular width increase with central meridian distance. The 3D propagation directions are similar to the flare locations. The angular width-speed relationship in 3D is much stronger than that in 2D.

1. Introduction

Coronal Mass Ejections (CMEs), especially front-side halo CMEs, are widely understood as one of major causes of heliospheric and geomagnetic disturbances that can influence the performance and reliability of modern technological systems (St. Cyr et al. 2000; Webb et al. 2000; Wang et al. 2002; Zhang et al. 2003; Kim et al. 2005; Moon et al. 2005; Michalek et al. 2007). To understand and forecast these disturbances in the interplanetary (IP) space caused by CMEs, it is essential to get their 3D parameters, such as speed, angular width, and propagation direction (Taktakishvili et al. 2009; Lugaz et al. 2011; Jang et al. 2014; Lee et al. 2014).

More than twenty thousand of CMEs have been observed after the launch of the Solar and Heliospheric Observatory (SOHO: 1997~), which moves around the Sun in step with the Earth, by slowly orbiting around the first Lagrangian Point (L1) approximately 1.5 million kilometers away from the Earth in the direction of the Sun (Domingo et al. 1995). Since the coronagraph images from the Large Angle Spectroscopic Coronagraph (LASCO; Brueckner et al. 1995) on board SOHO provides only projected two dimensional (2D) data, many researchers have attempted to obtain CME three dimensional (3D) parameters, by applying geometrical models such as cone models (Zhao et al. 2002; Xie et al. 2004; Xue et al. 2005; Michalek 2006) and the graduated cylindrical shell (GCS) model (Thernisien et al. 2006). Despite these effrts, there are still significant uncertainties in terms of angular width from single coronalgraph (Na et al. 2013).

Since its launch on 2007, the Solar TErrestrial RElations Observatory (STEREO) mission has provided a totally new perspective on solar eruptions by imaging CMEs and background events from twin spacecraft (Kaiser et al. 2008). These twin spacecraft enable us to observe CMEs in a stereoscopic way. Their data can be used to develop various geometrical methods based on dfferent assumptions (e.g., Thernisien et al. 2009; Liewer et al. 2009; Temmer et al. 2009; de Koning et al. 2009; Liu et al. 2010) in order to minimize the above uncertainties shown in 2D data analysis. Bosman et al. (2012) estimated the locations and angular widths of 51 well-identified STEREO CMEs from 2007 to 2010 by the GCS model. Shen et al. (2013) analyzed 86 full halo CMEs from March 2007 to May 2012 by applying the GCS model and estimated the projection effect by examining the ratio of 3D and 2D speed as a function of deviation angle. Mierla et al. (2010) compared several different techniques in terms of velocity and location using 5 events in 2007. Lee et al. (2015; submitted) evaluated 3D CME parameters using 44 halo CMEs when SOHO and STEREO were in quadrature from December 2010 to June 2011. They found that 3D parameters from STEREO CME analysis tool (StereoCAT) based on a triangulation method and GCS model are quite similar to each other.

In this paper, we use the StereoCAT to obtain the 3D CME parameters and present a comprehensive catalog of 308 front-side halo (partial and full) CMEs from 2009 to 2013 by both SOHO and STEREO. We compare 2D CME parameters from a single spacecraft (SOHO) and 3D ones from multi-spacecraft, which is the most comprehensive statistical comparison between them.

2. Data and Method

We investigate LASCO halo CMEs (apparent angular width ≥ 120°) from 2009 to 2013. Then, we choose 308 front-side halo CMEs, which are well-observed by both SOHO and STEREO. These CMEs have 2D parameters from single spacecraft and 3D ones from the multi-spacecraft. The 2D speed and angular width are directly taken from LASCO catalog (http://cdaw.gsfc.nasa.gov/CME_list/). We assume the 2D propagation directions of CMEs as the flare locations taken from NGDC flare catalog (http://www.ngdc.noaa.gov/stp/solar/solarares.html), which assume that the CMEs occur at the active region and propagate radially. If the location information is not available, we use SDO AIA (193 Å and 304 Å) and STEREO EUVI (195 Å and 304 Å) images to find bright features or any kind of eruption signatures.

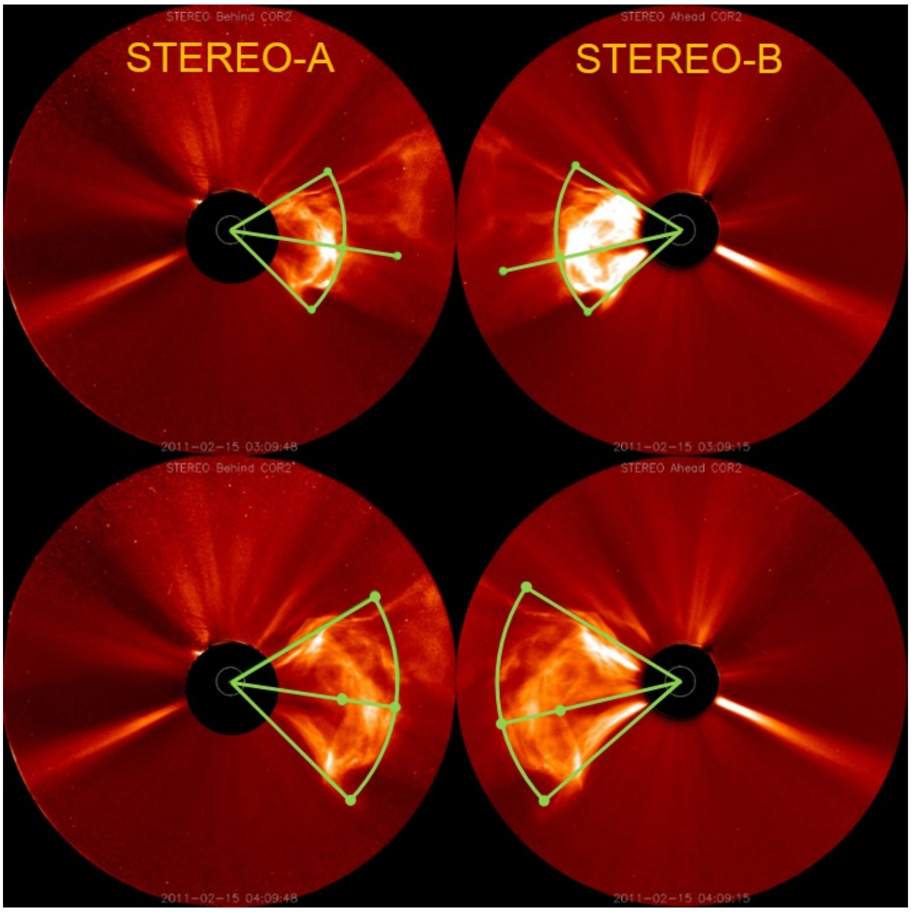

Figure 1. Snapshot of the CME on 15 Feb. 2011 by the STEREO Cat.

To determine the 3D CME parameters, we use the STEREO CME analysis tool (StereoCAT; http://ccmc.gsfc.nasa.gov/analysis/stereo/) based on a triangulation method, which is provided by NASA CCMC. This tool assumes that the angular width and propagation direction of a CME is fixed in coronagraph field of view. Figure 1 shows a snapshot of the CME on 15 Feb. 2011 by the StereoCAT. It is possible for us to choose two coronagraph images among three spacecraft: SOHO, STEREO A and B. There is more detailed information in website (http://ccmc.gsfc.nasa.gov/analysis/stereo/manual.pdf).

3. Result and Discussion

Figure 2 shows the histograms of 2D and 3D CME speed. For all CMEs, the mean value of 2D speed is 733 km/s, which is a little smaller than that (899 km/s) of 3D speed; 2D speeds tend to be about 20% underestimated when compared to 3D ones. It is probably due to the projection effect for single- coronagraph. For the 2D speeds of partial and full halo CMEs, their mean values are 614 km/s and 1032 km/s, respectively. We find that full halo CMEs are faster than the partial halo CMEs, which is consistent with Lara et al. (2006) who found that the speeds of halo CME (W_{2D} > 320°) are obviously higher than those of normal and partial halo CMEs. Similarly, Yashiro et al. (2004) also showed that the average 2D speed of halo CMEs is twice that of normal CMEs ($20° < W_{2D} < 120°$). This tendency is also found for 3D speeds, 750 km/s for partial halo CMEs and 1269 km/s for full halo CMEs.

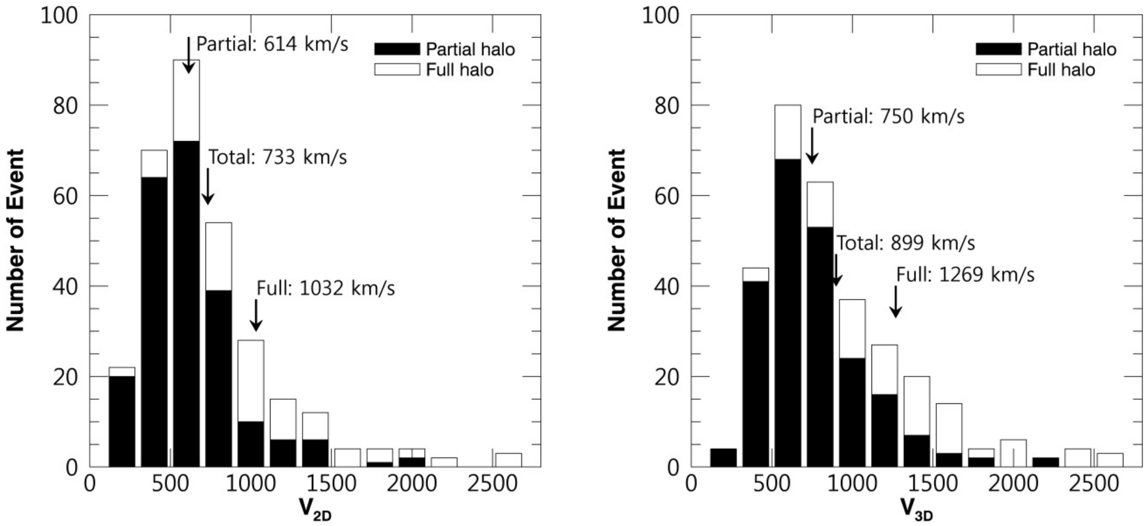

Figure 2. Histogram of 2D and 3D CME speeds.

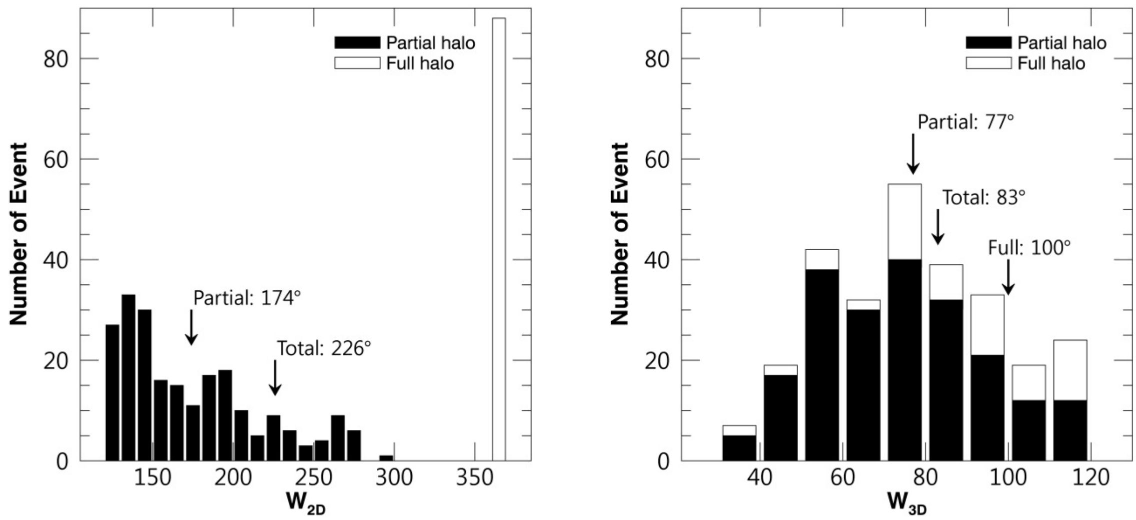

Figure 3. Histogram of 2D and 3D CME angular width.

Figure 3 shows the histograms of 2D and 3D angular width. The ranges of 2D and 3D angular width are very different from each other. The 2D angular width is larger than 120°, which is a criteria of our data selection. On the other hand, the 3D angular width ranges from 30° and 158° and closely follows a normal distribution with the mean values of 83°. Our results are almost similar to Michalek (2010) who evaluated that an average angular width for 69 halo CMEs from 2001 and 2002 using an asymmetric cone model is 83°. The mean value (100°) of the 3D angular width for the full halo CMEs is quite similar to Shen et al. (2013) who showed that the average value of the 3D angular width from the GCS model is 103°.

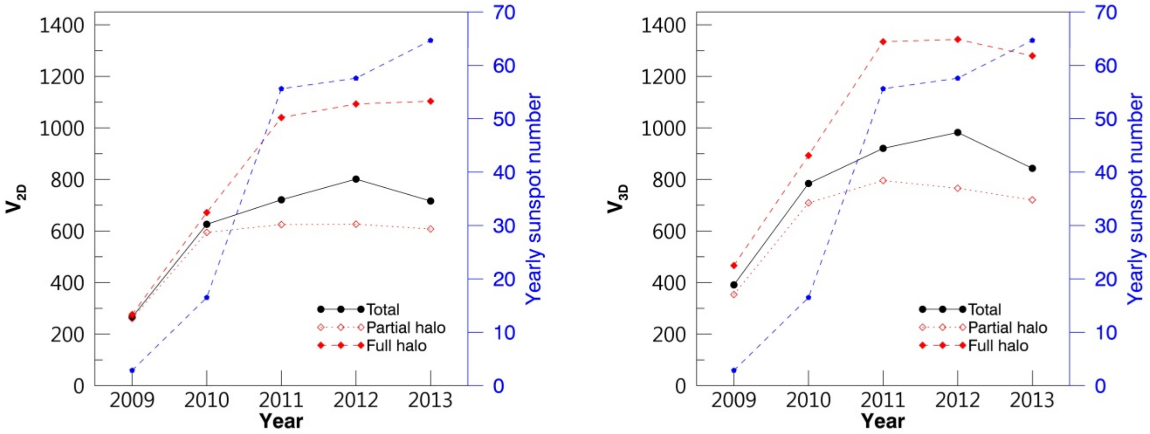

Figure 4. Yearly variation of 2D and 3D CME speed.

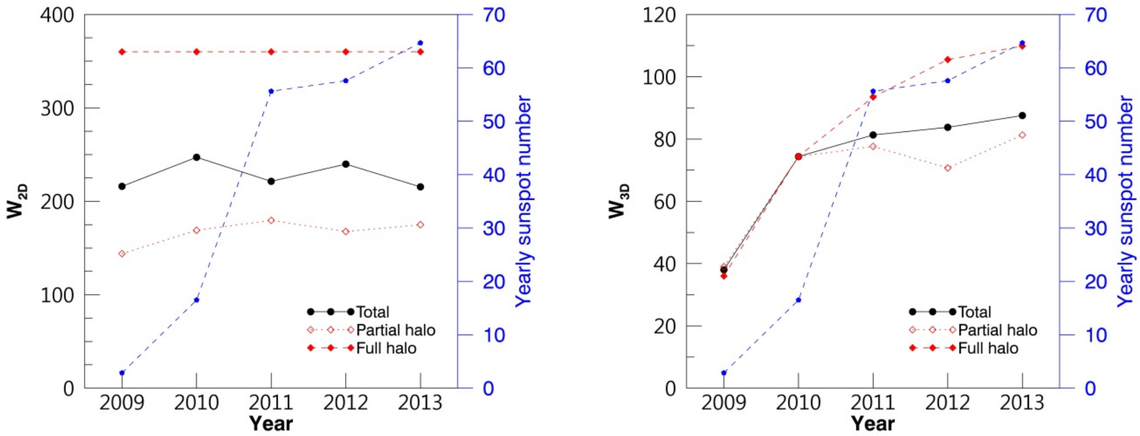

Figure 5. Yearly variation of 2D and 3D angular width.

We also show the yearly variation of CME speed in Figure 4. We include the yearly sunspot number to indicate solar activities. We find a tendency that 2D and 3D speeds increase up to 2013 that is generally considered as the maximum phase of solar cycle 24. Yashiro et al. (2004) showed that the 2D CME speed for normal CMEs varies from 320 km/s to 521 km/s in the time period 1996-2002, which is consistent with ours. It is noted that this trend is much clear in the full halo CMEs for both 2D and 3D speeds. A variation range of the 3D speed is about 400 - 1300 km/s, which is slightly larger than that (about 300 - 1100 km/s) of the 2D one. Because there are only 3 events in 2009, their statistical meaning is not so high.

In addition, we make an attempt to describe the yearly variation of angular width in Figure 5. There are no changes in the 2D CME angular width from 2009 to 2013. In the case of the partial halo CMEs, there is a slight increase (approximately 30°) with solar activity, which is similar to Yashiro et al. (2004) who found that the 2D angular width of the normal CMEs increase from 47° (solar minimum) to 61° (early phase of solar maximum). In contrast, the 3D angular width noticeably increases with solar activity. It is noted that the mean value of angular width for the full halo CMEs remarkably increases from 40° to 110°. This may be due to the projection effect of the 2D angular width. The 2D CME angular width is defined when it reaches maximum because it is gradually increases with time (Yashiro et al. 2004), which results in the overestimation of angular width. For this reason we cannot see a clear dependence of 2D angular width on solar cycle phase.

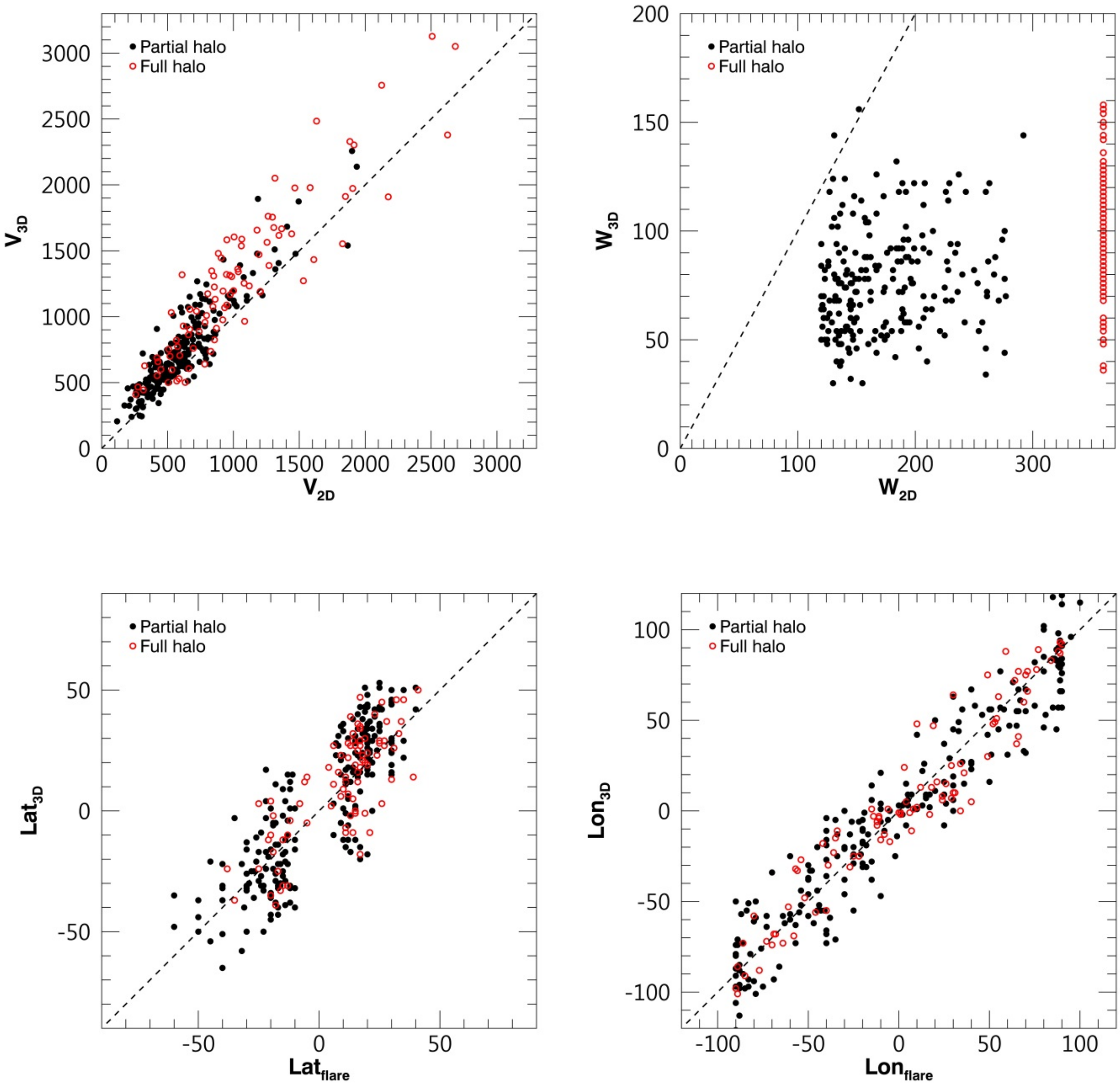

Figure 6. Scatterplots between 2D and 3D parameters.

Figure 6 shows scatterplots between 2D and 3D CME parameters such as speed, angular width, latitude, and longitude. To examine how two values are different, we calculate mean absolute difference (MAD) expressed by $\sum|P_{3D} - P_{2D}|/N$. For the speed, 2D and 3D values are similar to each other and the MAD value is 189 km/s. It is also shown that the 2D and 3D speeds of the full halo CME are higher than those of the partial halo CMEs. As shown in Figure 5b, the 3D angular width quite differs from the 2D one. Although there is a very weak tendency, we cannot find a clear correlation between 2D and 3D angular width, which seems to be due to the projection effect. For the latitude and longitude as shown in Figures 5c and d, the 2D and 3D values are similar to each other with the low MAD values (12.5° and 13.5°). It indicates that the most of CMEs statistically propagate radially although some CMEs are noticeably deflected.

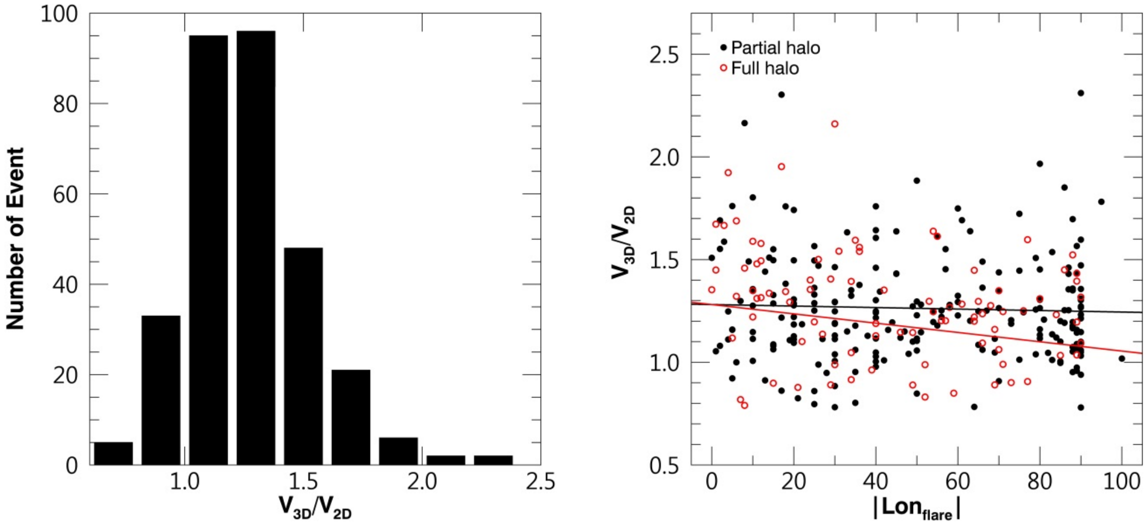

Figure 7. Histogram of the speed ratio (left) and its distribution as a function of longitude (right).

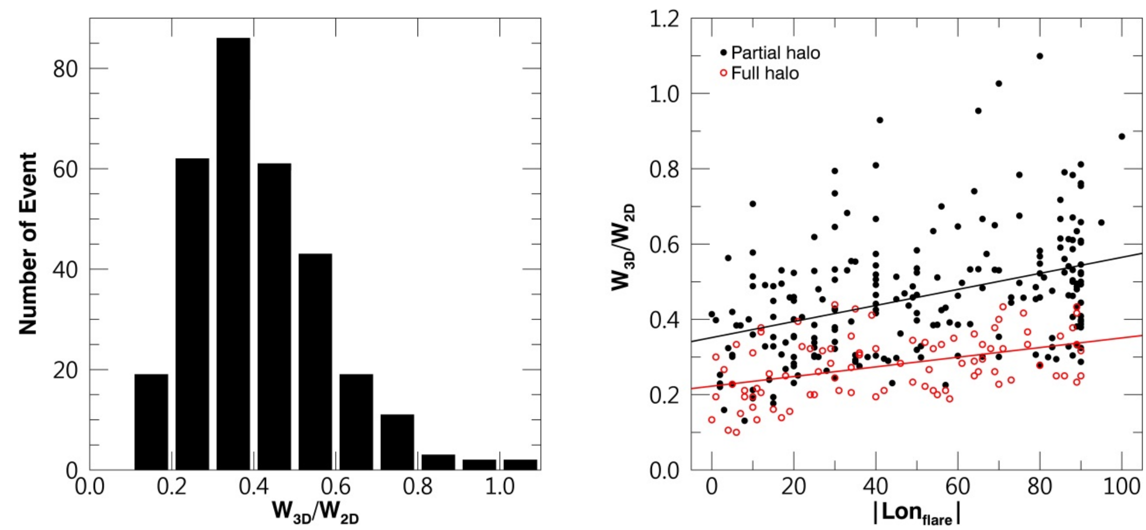

Figure 8. Histogram of the angular width ratio (left) and its distribution as a function of longitude (right).

We check a distribution of the speed ratio (V_{3D}/V_{2D}) and dependence on longitude to find the projection effect in Figure 7. Following Shen et al. (2013) who estimated that the error is about 0.2 Rs (about 4 pixel uncertainty in SOHO/LASCO C3 images), the mean values of the relative error of the 2D speed is about 10%. We also estimated about 10% error in 3D speed, which is determined by ten times trials of measurements. That means that the speed ratio roughly between 0.8 and 1.2 indicates that there is no projection effect. In this sense, 57% (175 out of 308) of the total events and 64% (56 out of 88) of the full halo CMEs have the projection effect (the speed ratio > 1.2). These percentages are much higher than Shen et al. (2013) found that 25% for the full halo CMEs (22 out of 88) have the projection effect. We also investigate the angular width ratio (W_{2D}/W_{3D}) in Figure 9. The ratio of the most events is much smaller than the unity and it means that the 2D angular width is quite underestimated because of the projection effect. The angular with ratio is lower when CMEs are appeared around solar center and look like full halo types.

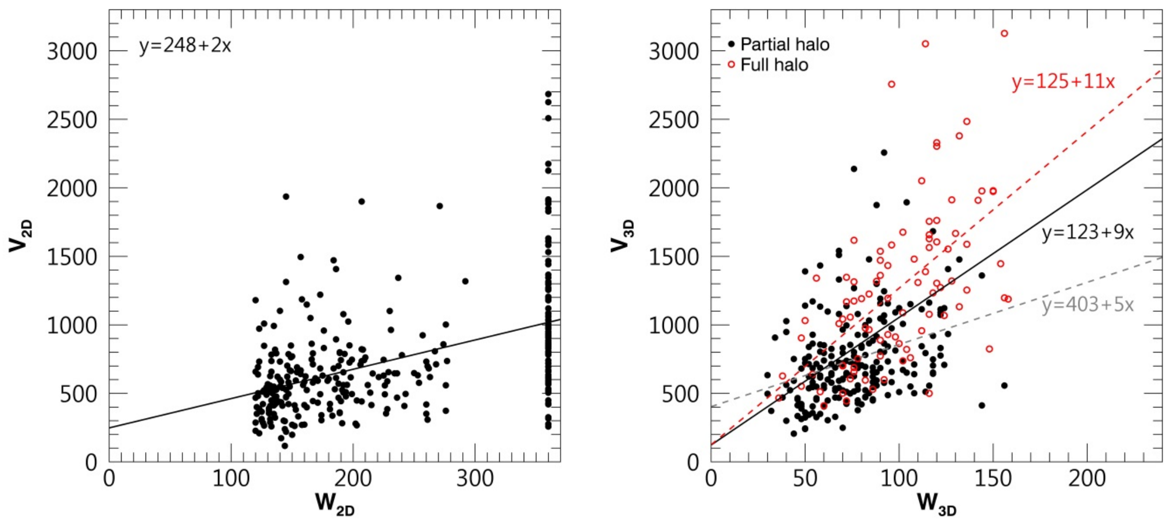

Figure 9. The relationship between angular width and speed in 2D (left) and 3D (right).

Additionally, we show the relationship between angular width and speed in Figure 7. The relationship in 2D shows that wider CMEs have a tendency to be fast. A correlation coefficient between of them is 0.47, which is similar to the previous studies by Yashiro et al. (2004), Vrsnak et al. (2007) and Howard et al. (2008). It is noted that this trend is much clear in 3D values (CC~0.54) and the slope of the 3D values is four times steep compared the 2D ones. Especially, this tendency of the full halo CMEs is much stronger with higher correlation (CC~0.58) with the steeper slope.

4. Summary and Conclusion

We have made a comprehensive catalog of 308 front-side halo CMEs (apparent angular width ≥ 120°) observed by both SOHO and STEREO from 2009 to 2013, which is available by the request to the authors. This is the first comprehensive CME catalogue which includes 3D CME parameters: speed, angular width, and propagation direction. We use the StereoCAT to obtain the 3D CME parameters. Our major results from this study can be summarized as follows. First, 2D speed is approximately 20% underestimated and the 2D angular width is remarkably overestimated due to the projection effect. Second, 3D speed and angular width increase with solar activity. Third, 3D propagation direction are similar to the flare location. Forth, the CMEs that occurred at solar center obviously have the projection effect in terms of speed and angular width.

In 2015, STEREO A and B do not provide us with data because the former is in safe mode for superior solar conjunction and the latter has a telemetry problem. Stereoscopic observations of ours and other results (Gopalswamy et al. 2012; Shen et al. 2013) show that the 3D angular width of the CME quite differs from the projected 2D one. To estimate the 3D CME morphology, there are many models using multi-spacecraft data (the STEREO Cat, GCS model) and single-spacecraft data (cone models). Lee et al. (2015 submitted) compared the CME 3D parameters calculated by three models, such as StereoCAT, the GCS model, and the asymmetric cone model, using the halo CMEs observed from Dec. 2010 to Jun. 2011. They direct observed the CME speed and angular width without projection effect because SOHO and STEREO spacecraft were in quadrature at that period. They found that the 3D speed and propagation direction using the three models are similar to direct observations except the 3D angular width. The 3D angular width for the asymmetric cone model tends to overestimate than direct observation. Therefore it is necessary to observe the CMEs via multi-spacecraft to estimate the 3D angular width accurately.

5. References

Bosman et al., 2012, Sol. Phys., 281, 167-185

Brueckner et al., 1995, Sol. Phys., 162, 357-402

de Koning et al., 2009, Sol. Phys., 256, 167181

Domingo et al., 1995, Sol. Phys., 162, 137

Gopalswamy et al., 2012, Sun and Geophere, 7(1), 7-11

Howard et al., 2008, J. Geophys. Res., 113, A01104

Jang et al., 2014, J. Geophys. Res., 119, 71207127

Kim et al., 2005, J. Geophys. Res., 110, A11104

Kaiser et al., 2008, Space Sci. Rev., 136, 5-16

Lara et al., 2006, J. Geophys. Res., 111, A06107

Liewer et al., 2009, ApJ, 772, 1762-1777

Liu et al., 2010, Sol. Phys., 256, 55-72

Lee et al., 2014, Sol. Phys., 289(6), 2233-2245

Lugaz et al., 2011, Advances in Space Research, 48, 292-299

Moon et al., 2005, ApJ, 624, 414-419

Michalek, 2006, Sol. Phys., 237, 101-118

Michalek, et al., 2007, Sol. Phys., 246, 399-408

Michalek, 2010, Sol. Phys., 261, 107114

Mierla et al., 2010, Ann. Geophys., 28, 203-215

Na et al., 2013, Sol. Phys., 288, 313-329

Shen et al., 2013, J. Geophys. Res., 118, 6858-6865

St. Cyr, O. C. et al., 2000, J. Geophys. Res., 105(A8), 18169-18185

Taktakishvili et al., 2009, Space Weather, 7, S03004

Temmer et al., 2009, Sol. Phys., 256, 183-199

Thernisien et al., 2006, ApJ, 652, 763-773

Thernisien et al., 2009, Sol. Phys., 256, 111-130

Vrsnak et al., 2007, A&A 269, 339-346

Wang, Y. M. et al., 2002, J. Geophys. Res., 107(A11), 1340

Webb, D. F. et al., 2000, J. Geophys. Res., 105(A4), 7491-7508

Xie et al., 2004 J. Geophys. Res., 109, A03109

Xue et al., 2005, J. Geophys. Res., 110, A08103

Yashiro et al., 2004, J. Geophys. Res., 109, A07105

Zhang et al., 2003, ApJ, 582, 520-533

Zhao et al., 2002, J. Geophys. Res., 107(A8), 122